

Molecular Level Structural Heterogeneity in Poly(ether–ester)/Poly(vinyl chloride) Blend Characterized by Cross-Polarization/Magic Angle Spinning ^{13}C Nuclear Magnetic Resonance Spectroscopy

Seung-Yeop Kwak,* Jae-Jin Kim, and Un Young Kim

Division of Polymer Research, Korea Institute of Science and Technology, P.O. Box 131, Cheongryang, Seoul 130-650, Korea

Received September 21, 1995; Revised Manuscript Received January 25, 1996[®]

ABSTRACT: A blend of poly(ether–ester) and poly(vinyl chloride) (PVC) was examined by dynamic mechanical analysis and cross-polarization/magic angle spinning (CP/MAS) ^{13}C NMR spectroscopy. The presence of structural heterogeneity in the solid blend was identified by the temperature dependence of its frequency-swept viscoelastic behavior. In the CP/MAS ^{13}C NMR experiment, analysis of the magnetization decay of specific carbons as a function of delay time determined the proton spin–lattice relaxation times in the laboratory frame, T_1 , and the rotating frame, $T_{1\rho}$, for the two polymers in their respective pure states and in the 50/50 blend. This analysis provided more precise information pertaining to the microheterogeneity and the molecular state of mixing in the blend. The single-exponential decay of T_1 relaxation of the blend confirmed a homogeneity on a characteristic length of 26 nm estimated from the spin diffusion process. The double decompositions in the $T_{1\rho}$ relaxation of component polymers in the blend indicated a coexistence of a mixed and two structurally heterogeneous phases which corresponded to poly(ether–ester) hard segments and PVC microcrystallites. The maximum size of the microheterogeneous phases was estimated to be *ca.* 24 Å.

Introduction

Poly(ether–ester) is a copolymer consisting of random sequences of poly(tetramethylene ether) glycol terephthalate and poly(tetramethylene) terephthalate blocks.^{1,2} The former forms amorphous soft segments and are rubbery down to low temperatures.³ The microphase separation of the latter into crystalline domains produces hard segments serving as thermally reversible physical cross-links. Due to the heterophase nature, poly(ether–ester) is a thermoplastic elastomer which has the unique properties of vulcanized rubbers coupled with the processing characteristics of conventional thermoplastics. Poly(vinyl chloride) (PVC), suspension grade, is a powder of about 100–150 μm grains and consists of unique hierarchical structure of skins and tight agglomerates ($\sim 10\ \mu\text{m}$); the agglomerate is composed of primary particles ($\sim 1\ \mu\text{m}$) which in turn consist of domains ($\sim 0.1\ \mu\text{m}$); the domain is made up of microdomains ($\sim 10\ \text{nm}$) held internally by microcrystallites. These microcrystallites act as physical cross-links and preserve the strength of PVC.^{4–6} According to Lundberg,⁷ PVC is considered to be a thermoplastic elastomer in a broad sense because of the distribution of microcrystallites as a hard phase throughout the amorphous chains as a soft phase. It is understood that the high modulus and strength of the two polymers result from the presence of structural heterogeneity, *i.e.*, hard phases.

Blends of poly(ether–ester) and PVC have gained much interest because they provide not only improved physical/mechanical properties but also diverse characteristics from different blend ratios of commercially available grades. In addition, they also provide optimum cost-performance balance in various engineering applications.⁸ Nishi *et al.*^{9,10} have studied the poly(ether–ester)/PVC blends and reported an occurrence

of extensive mixing between amorphous chains of two polymers. They also indicated that in the heat-treated sample microheterogeneous structures existed in the order of or less than 10 nm; however, their nascence and identity remain unclear.

The objective of this study is to acquire detailed molecular level information about the identity and size of structural heterogeneity as well as the state of homogeneity in the solid blend of poly(ether–ester)/PVC (50/50 mass ratio), recognizing that structural heterogeneity and the state of mixing in a given blend system govern the physical/mechanical properties and that most polymer blends find their actual end use in the solid state. First, the presence of the structural heterogeneity in this blend is detected by the temperature dependence of frequency-swept dynamic mechanical properties; the information obtained is indirect and qualitative. Second, a more precise and quantitative information on the molecular state of the solid phase is sought with high-resolution, pulsed Fourier-transformed (FT) ^{13}C nuclear magnetic resonance (NMR) spectroscopy capable of magic angle spinning (MAS) and cross-polarization (CP). In the CP/MAS ^{13}C NMR, the naturally rare ^{13}C spins are polarized through the dipolar coupling with the abundant ^1H spins and the magnetization of the ^1H is transferred to the ^{13}C . This brings about significant enhancement of ^{13}C signal intensity and reduction in data acquisition time.¹¹ Moreover, the MAS contributes to remove the heteronuclear dipole–dipole interactions and the chemical shift anisotropy, thereby narrowing the line widths of the spectrum; the resonance of carbons attached to the different nuclear environments can be resolved.¹² Measurements of the proton spin–lattice relaxation times for the specific carbons in the blend permit an analysis and identification of the microheterogeneous structures in terms of the difference in their relaxation behavior.^{13–16} Furthermore, the spatial dimensions of the heterophase domains can be evaluated^{13–16} by an approximate approach based on the spin diffusion phenomenon.^{17,18}

* To whom correspondence should be addressed.

[®] Abstract published in *Advance ACS Abstracts*, April 1, 1996.

Depending on the use of the relaxation times in the laboratory frame, T_1 , and the rotating frame, $T_{1\rho}$, the heterophase domains are characterized at two size levels having a difference by 1 order of magnitude.

Experimental Section

Materials and Blend Preparation. Poly(ether-ester) (Hytrel 4056) was obtained in pellet form from E. I. DuPont de Nemours & Co. The soft segments of this polymer, poly-(tetramethyl ether) glycol terephthalate, has a number-average molecular weight of about 1000.¹⁹ The hard segments, poly-tetramethylene terephthalate, are about 6 units long on the average and consist of *ca.* 44 wt % polymer.^{20,21} The overall number-average molecular weight is about 30 000, and the glass transition and melting temperatures are *ca.* -50 and *ca.* 150 °C, respectively.²² PVC resin (Geon 103 EP F-76) was supplied by Geon Co. Its number- and weight-average molecular weights are 40 000 and 89 000, respectively.²³

The two polymers were mixed in a batch internal mixer with nonintermeshing, counterrotating two-wing rotors (1.57 L Farrel Banbury mixer); the mass ratio was 50/50 and 1 phr of thermal stabilizer (Therm-Chek 1872 from Ferro Corp.) for PVC was incorporated. Before mixing, poly(ether-ester) was first masticated until a temperature of 135 °C. PVC was then charged into the chamber and the mixing continued for 450 s with a fill factor of 0.7 and a rotor speed of 80 rpm. After the completion of mixing, the batch of the blend was sheeted out through a two-roll mill. The sheets were compression molded and punched out with 25 mm diameter for the dynamic mechanical measurements or chopped into small pieces of about 1 mm \times 1 mm for the NMR experiments.

Frequency-Swept Dynamic Mechanical Measurements. The dynamic mechanical properties of the blend were measured with a Rheometrics RMS-800 mechanical spectrometer in dynamic shear oscillatory mode using 25 mm diameter parallel discs. The range of angular frequency was from $\omega = 10^{-1}$ to 10^2 rad/s. The temperature range was limited to where neither slippage between the surfaces of sample and disk nor thermal degradation took place. The strain amplitude was selected to be large enough for accurate torque signals and small enough to keep the material response in the linear region.

CP/MAS ^{13}C NMR Relaxation Measurements. The ^{13}C NMR experiments were performed with a Chemagnetic CMX-300 spectrometer (299.6 MHz for ^1H) equipped with a magic angle spinning probe. The sample was packed in zirconia rotors with Kel-F end caps and spun at a rate of about 3.5 kHz. A ^1H 90° pulse width of 4.25 μs was employed with *ca.* 5000 fid signal accumulations. T_1 relaxation times were measured by monitoring the decay of specific carbon peak intensities after π - τ - $\pi/2$ (inversion-recovery) pulse sequence followed by the cross-polarization, Figure 1a. $T_{1\rho}$ relaxation times were determined by applying ^1H spin-lock- τ pulse sequence prior to CP, Figure 1b, and then analyzing the resonance intensities. The CP Hartmann-Hahn contact time of 1 ms was taken.

Results and Discussion

Figure 2 shows the dynamic mechanical behavior of poly(ether-ester)/PVC blend at the corresponding temperature range. The data of storage modulus (G') and loss modulus (G'') at the same value of ω are plotted as locus form of $\log G''(\omega)$ vs $\log G'(\omega)$. As the temperature is increased from 100 to 175 °C, the $\log G''(\omega)$ vs $\log G'(\omega)$ curves show temperature dependence by shifting from right to left of the figure. This pattern indicates that the time-temperature correspondence is not applicable, and there must be a structural change.²⁴ Recognizing that the microcrystallites of PVC melt over a broad temperature range of 120–210 °C²⁵ and the melting of the hard-segment crystallites of poly(ether-ester) starts at *ca.* 150 °C, the structural change is attributable to the melting of crystallites of both poly-

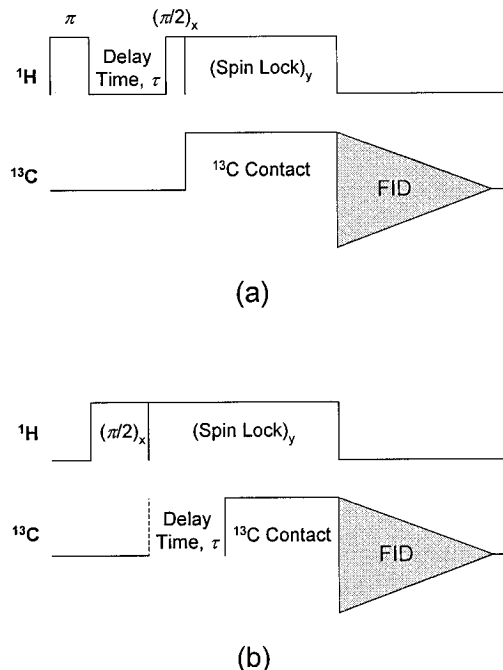


Figure 1. Pulse sequences used to determine proton spin-lattice relaxation times: (a) T_1 and (b) $T_{1\rho}$.

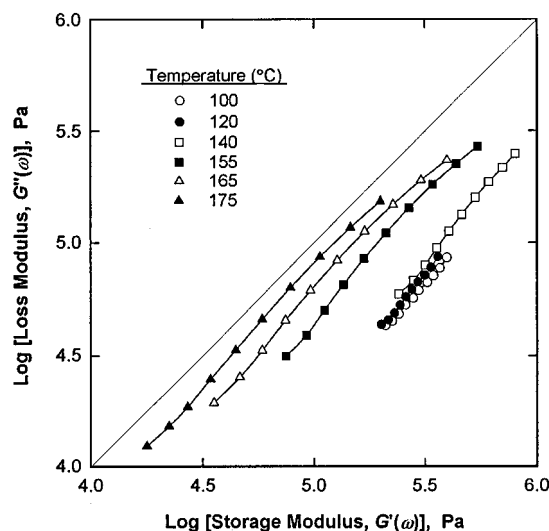


Figure 2. $\log G''(\omega)$ vs $\log G'(\omega)$ plots of poly(ether-ester)/PVC blend.

mers. Conversely, the melting of crystallites at higher temperatures assures, although indirect, a presence of structural heterogeneity in the solid blend. However, it is difficult to discern the structural heterogeneity that originates from the poly(ether-ester) fraction and that from the PVC fraction in the blend because the contribution of melting of individual crystallites to the $\log G''(\omega)$ vs $\log G'(\omega)$ curves can not be resolved.

Figure 3 contains CP/MAS ^{13}C NMR spectra of poly(ether-ester), PVC, and their blend (50/50) recorded at 21 °C. The spectrum of poly(ether-ester) consists of resonances at 27 ppm which arise from overlapping central CH_2 carbons of both soft and hard segments, at 65 and 70 ppm from OCH_2 carbons of hard and soft segments, respectively, at 130 and 134 ppm due to protonated and nonprotonated aromatic carbons, respectively, and at 165 ppm designated to carbonyl carbons. In the PVC spectrum, the methylene and methine carbon resonances are assigned to the resonances at 46 and 57 ppm, respectively. The spectrum

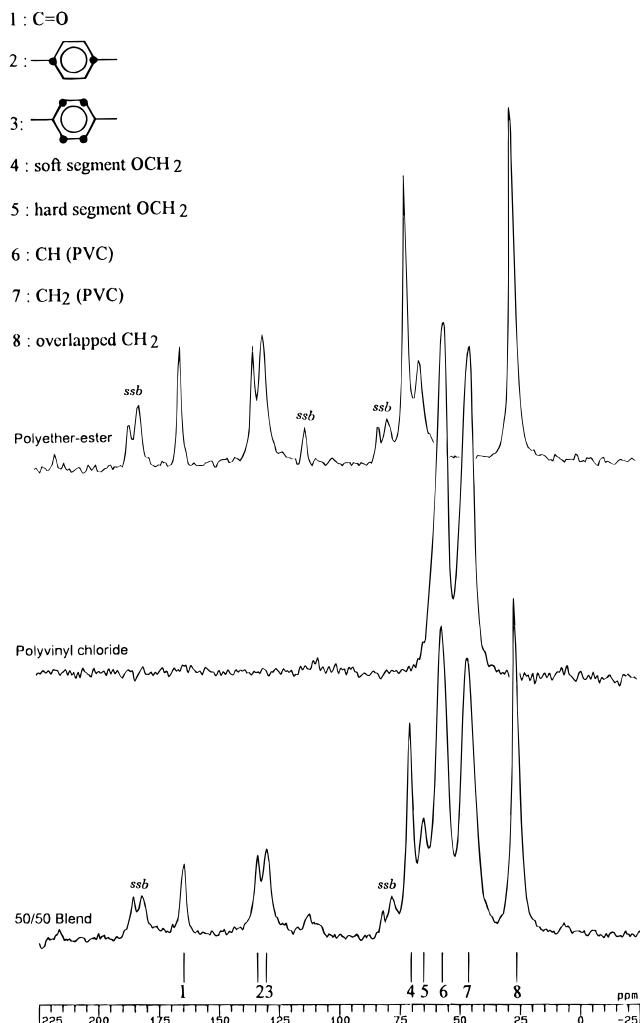


Figure 3. CP/MAS ^{13}C NMR spectra of poly(ether-ester), PVC, and their 50/50 blend. The spinning side band is labeled ssb.

of the blend is no more than a superposition of the spectra from the poly(ether-ester) and PVC. Among the carbons, the internal methylene (with no oxygen link) carbons of poly(ether-ester) and the methylene carbons of PVC in their pure and unblended state were selected to measure the proton spin-lattice relaxation times.

Figure 4 shows a plot of the ^{13}C resonance intensity of methylene carbons of poly(ether-ester) vs delay time for the measurement of ^1H T_1 's. The resonance intensity, assuming a perfect π pulse in Figure 1a, decays exponentially in concert with the proton magnetization with a time constant equal to the T_1 , as follows,

$$M(\tau) = M_\infty [1 - 2 \exp(-\tau/T_1)] \quad (1)$$

Taking the natural logarithm of both sides of eq 1 gives

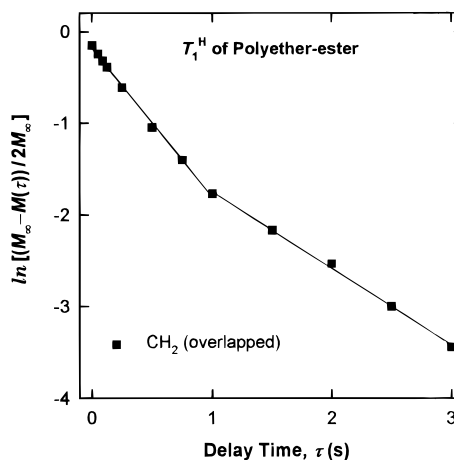


Figure 4. Logarithmic plot of ^{13}C resonance intensity vs delay time for poly(ether-ester) to measure proton T_1 .

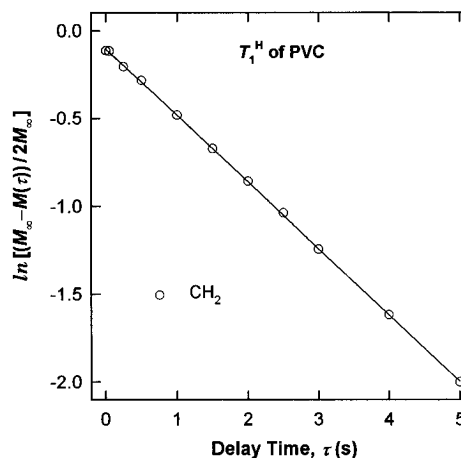


Figure 5. Logarithmic plot of ^{13}C resonance intensity vs delay time for PVC to measure proton T_1 .

$$\ln[M_\infty - M(\tau)] = -\tau/T_1 + \ln(2M_\infty) \quad (2)$$

with M_∞ as the intensity of the signal at $\tau \geq 5T_1$. Thus, a plot of $\ln[(M_\infty - M(\tau))/2M_\infty]$ against τ is expressed in Figure 4, indicating a double-component T_1 relaxation behavior. The slopes of the individual straight lines portion the T_1 's, listed in Table 1. The short component with considerably shorter T_1 is for a more rigid phase (hard segments), and the long component is for a more mobile phase (soft segments), which implies a phase-separated material. This observation indicates that the spin diffusion within the proton nuclear spin system is not effective enough to average out the T_1 's to a single value.

The logarithm of the ^{13}C signal intensity vs delay time for PVC, Figure 5, indicates a linear plot with a single value of T_1 , which implies that the material is homogeneous on the time scale over which the spin energy diffuses in the T_1 times.

Table 1. Results of Proton T_1 and $T_{1\rho}$ Measurements for Poly(ether-ester), PVC, and Their 50/50 Blend

carbon		^1H T_1 relaxation		^1H $T_{1\rho}$ relaxation	
		slope	T_1 (s)	slope	$T_{1\rho}$ (ms)
poly(ether-ester)	CH_2	-1.6299 (short component)	0.61	-0.4640 (short component)	2.16
		-0.8336 (long component)	1.20	-0.2908 (long component)	3.44
PVC	CH_2	-0.3785	2.64	-0.1948 (short component)	5.13
				-0.0937 (long component)	10.67
blend (50/50)	CH_2 (PVC fraction)	-0.8997	1.11	-0.2021 (short component)	4.95
				-0.1038 (long component)	9.63
	CH_2 (poly(ether-ester) fraction)	-0.9217	1.09	-0.3002 (short component)	3.33
				-0.1033 (long component)	9.68

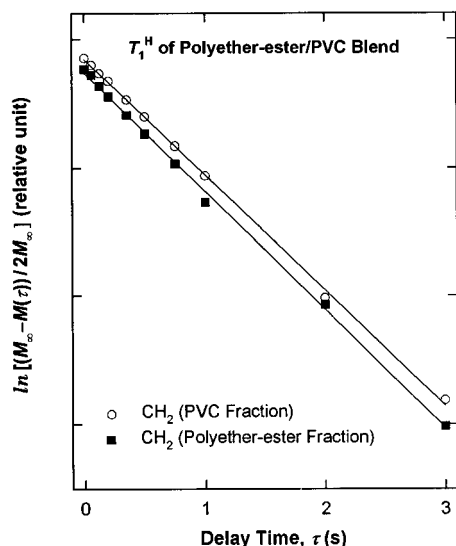


Figure 6. Logarithmic plots of ^{13}C resonance intensity vs delay time for poly(ether-ester)/PVC blend to measure proton T_1 .

Figure 6 shows T_1 relaxation behavior of the 50/50 blend. The logarithmic plots of the individual component fractions are linear and consistent with an identical T_1 , as indicated in Table 1. The identical T_1 value means that the protons of the constituent polymers relax at an average rate and are considered to be in the homogeneous environment.²⁶ Noteworthy, the change of T_1 relaxation behavior of poly(ether-ester) from double-component decay in the pure state to single-component decay upon blending indicates that the hard segments were affected by the PVC amorphous chains on blending, confirming the occurrence of a considerable mixing. From the single T_1 value of the blend, one can estimate the scale of mixing by the average diffusive path length, $\langle r \rangle$, for the effective spin diffusion, given by the following equation:^{18,27}

$$\langle r \rangle = (6DT)^{1/2} \quad (3)$$

The D is the spin diffusion coefficient determined by the average proton-to-proton distance and the strength of the dipolar interaction; it has typically a value of about $10^{-12} \text{ cm}^2 \text{ s}^{-1}$. The T is the characteristic time over which the spin diffusion proceeds and has the value of the T_1 in this case. Therefore, it is concluded that the two polymers are intimately mixed on a scale of *ca.* 26 nm.

The proton $T_{1\rho}$'s for poly(ether-ester) and PVC in their respective pure states and in the 50/50 blend were measured from decaying methylene carbon signals obtained in the delayed-contact ^{13}C CP/MAS experiment, Figure 1b, where various delay times are introduced between the $\pi/2$ pulse and the spin-lock pulse. The carbon resonance intensity decays with a time constant equal to the $T_{1\rho}$ by an exponential function:

$$M(\tau) = M_0 \exp(-\tau/T_{1\rho}) \quad (4)$$

Thus, the slope of a logarithmic plot of the magnetization intensity, $M(\tau)$, vs delay time, τ , yields the proton $T_{1\rho}$ value. It is understood that the rate of spin diffusion in the $T_{1\rho}$ relaxation is influenced by a shorter range of spatial proximity than that in the T_1 relaxation so that the state of solid phase is assessed more locally by roughly 1 order of magnitude.^{26,27}

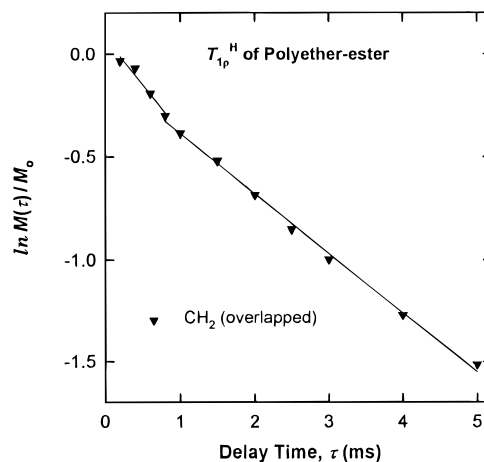


Figure 7. Logarithmic plot of ^{13}C resonance intensity vs delay time for poly(ether-ester) to measure proton $T_{1\rho}$.

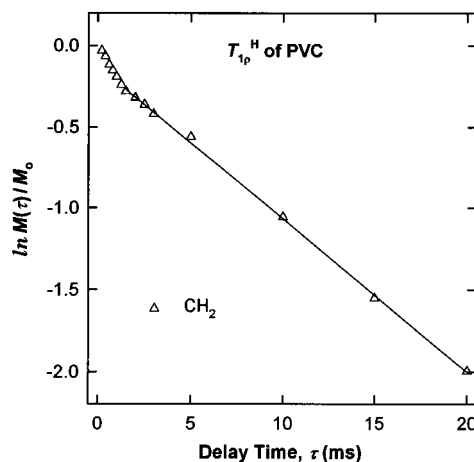


Figure 8. Logarithmic plot of ^{13}C resonance intensity vs delay time for PVC to measure proton $T_{1\rho}$.

For the pure poly(ether-ester), a double-component $T_{1\rho}$ decay process was observed as indicated by the slope change in the $\ln M(\tau)/M_0$ vs τ plot in Figure 7. The slope at the shorter delay times yields a $T_{1\rho}$ for a hard phase, while that at the longer times results in $T_{1\rho}$ for an amorphous soft phase, as listed in Table 1. Considering that the lamellar crystalline region of hard segments seemed to exceed the range for the $T_{1\rho}$ probe to be effective and a substantial fraction of isolated phases consisting of uncrystallized hard-segment units resides in the elastomeric phase,^{21,28-30} the above $T_{1\rho}$ favors to be pertinent to the isolated phases. A double-component $T_{1\rho}$ relaxation also occurred in the pure PVC, shown in Figure 8. In Table 1, the shorter $T_{1\rho}$ belongs to the microcrystallites, and the longer one indicates the amorphous chains.

Figure 9 represents the $T_{1\rho}$ relaxation behavior of the blend, monitored from decaying methylene carbons of the component polymer fractions. Both plots show a double-exponential decay relaxed with the corresponding time constants, $T_{1\rho}$'s, as summarized in Table 1. By using the $T_{1\rho}$ values for the blend, in conjunction with the $T_{1\rho}$ or T_1 for the pure polymers, it may be possible to assess the microscopic state of phase morphology and, further, to estimate the size of heterogeneity in the blend. The $T_{1\rho}$'s of the long components of the blend were identical for both fractions and intermediate in value as compared to those of the unblended polymers. This observation reveals a tight coupling in the proton spin system of the blend, thus a homogeneous phase on

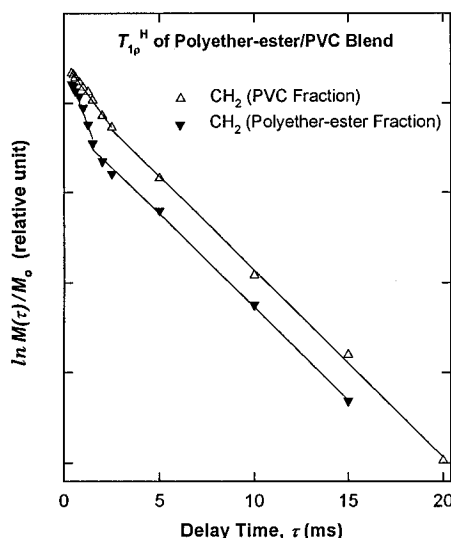


Figure 9. Logarithmic plot of ^{13}C resonance intensity vs delay time for poly(ether-ester)/PVC blend to measure proton $T_{1\rho}$.

the scale covered by the spin diffusion. In contrast, the blend $T_{1\rho}$'s of the short components are dependent on the selected carbons, indicating an inefficient dipolar coupling and hence a presence of structural heterogeneity. Overall, the $T_{1\rho}$ results suggest that the blend is composed of (i) a mixed phase of poly(ether-ester) and PVC amorphous chains, (ii) PVC microcrystalline phase, and (iii) poly(ether-ester) crystalline domains. The short-component $T_{1\rho}$ of PVC in the blend is slightly shorter than that of pure PVC. Evidently, the microcrystallites of PVC were somewhat influenced by the poly(ether-ester) upon blending. In comparison of the short-component $T_{1\rho}$ of poly(ether-ester) in the blend to the short-component T_1 of the pure polymer, the size reduction of the crystallites during blending is observed to be much more obvious relative to PVC. Recognizing that it is possible to estimate the upper limit to the microseparated domains from the relaxation times with single-component decay through the application of eq 3, the identical $T_{1\rho}$ value (ca. 9.7 ms) at longer delay times in the blend led to an estimate of the maximum domain size of 24 Å, at which magnetization transport is effective to permit a rapid diffusion for the proton spins. The above size estimate, however, is approximate because the value of the spin diffusion coefficient, D , has not been exactly measured.

On the basis of information on the structural heterogeneity obtained in this study, the structure-property relationships of this blend, i.e., the effect of microheterogeneous structures on the large deformational viscoelastic behavior, will be the subject of the future publication.

Conclusions

The combined results obtained by dynamic viscoelastic measurements and CP/MAS ^{13}C NMR analysis with proton T_1 and $T_{1\rho}$ measurements provided a clear insight into the structural heterogeneity and state of homogenization of poly(ether-ester)/PVC blend. The log $G''(\omega)$ vs log $G'(\omega)$ plots of the dynamic viscoelastic data indicated that the structural heterogeneity from the crystalline phases of the component polymers was present, as revealed by the temperature dependence of the plots due to the melting of the crystallites with increasing temperature. On the basis of a single-

exponential decay of T_1 relaxation behavior of the blend and an identical T_1 value of the component polymers, it was concluded that the respective chains of poly(ether-ester) and PVC were in intimate contact and homogeneous mixing occurred on a scale of ca. 26 nm. Separate detection of a double-exponential decay of $T_{1\rho}$ relaxation and analysis of the corresponding $T_{1\rho}$ times in the individual blend components confirmed the existence of three phases consisting of a mixed and the structural heterophases of poly(ether-ester) and PVC microcrystallites. The size reduction of the heterophases, relative to the pure states, implied that the crystallites of the two polymers were affected more or less upon blending. The maximum scale of the heterophases was approximately quantified to be 24 Å.

Acknowledgment. It is a pleasure to acknowledge the helpful discussion with Professor N. Nakajima at The University of Akron. The authors are grateful to the Korea Institute of Science and Technology (KIST) for the support of this work.

References and Notes

- Witsiepe, W. K. In *Polymerization Reactions and New Polymers*; Platzner, N. A. J., Ed.; Adv. Chem. Ser. 129; American Chemical Society: Washington, DC, 1973; Chapter 4.
- Hoeschele, G. K.; Witsiepe, W. K. *Angew. Makromol. Chem.* **1973**, 29/30, 267.
- Cellar, R. J. *J. Polym. Sci.: Symp.* **1973**, 42, 727.
- Geil, P. H. *J. Macromol. Sci.-Phys.* **1977**, B14, 171.
- Butters, G., Ed. *Particulate Nature of PVC*; Applied Science: London, 1982.
- Munstedt, H. *J. Macromol. Sci.-Phys.* **1977**, B14, 195.
- Lundberg, R. D. In *Handbook of Thermoplastic Elastomers*; Walker, B. M., Ed.; Van Nostrand Reinhold: New York, 1979; p 247.
- Kane, R. P. *J. Elast. Plast.* **1977**, 9, 416.
- Nishi, T.; Kwei, T. K.; Wang, T. T. *J. Appl. Phys.* **1975**, 46, 4157.
- Nishi, T.; Kwei, T. K. *J. Appl. Polym. Sci.* **1976**, 20, 1331.
- Hartmann, S. R.; Hahn, E. L. *Phys. Rev.* **1962**, 128, 2042.
- Schaefer, J.; Stejskal, E. O. *J. Chem. Soc.* **1976**, 98, 1032.
- McBrierty, V. J.; Douglass, D. C. *J. Polym. Sci., Macromol. Rev.* **1981**, 16, 295.
- Linder, M.; Hendrichs, P. M.; Hewitt, J. M.; Massa, P. J. *J. Chem. Phys.* **1985**, 82, 1585.
- Parmer, J. F.; Dickenson, L. C.; Chien, J. C. W.; Porter, R. S. *Macromolecules* **1989**, 22, 1078.
- Masson, J.-F.; Manley, R. St. J. *Macromolecules* **1991**, 24, 6670.
- McBrierty, V. J.; Douglass, D. C. *Phys. Rep.* **1989**, 63, 61.
- McBrierty, V. J.; Packer, K. J. *Nuclear Magnetic Resonance in Solid Polymers*; Cambridge University Press: Cambridge, U.K., 1993.
- Wolf, J. R., Jr. *Polym. Prepr. (Am. Chem. Soc., Div. Polym. Chem.)* **1978**, 19, 5.
- Jelinski, L. W.; Schilling, F. C.; Bovey, F. A. *Macromolecules* **1981**, 14, 581.
- Cellar, R. J. *Encycl. Polym. Sci. Technol., Suppl.* **1977**, 2, 485.
- Buck, W. H.; Cellar, R. J.; Gladding, E. K.; Wolf, J. R., Jr. *J. Polym. Sci.: Symp.* **1974**, 48, 47.
- Daniels, C. A.; Collins, E. A. *J. Macromol. Sci.-Phys.* **1974**, B10, 287.
- Nakajima, N.; Kwak, S.-Y. *Int. Polym. Proc.* **1995**, 10, 24.
- Witenhafer, D. E. *J. Macromol. Sci.-Phys.* **1970**, B4, 915.
- Dickinson, L. C.; Yang, H.; Chu, C.-W.; Stein, R. S.; Chien, J. C. W. *Macromolecules* **1987**, 20, 1757.
- McBrierty, V. J.; Douglass, D. C.; Kwei, T. K. *Macromolecules* **1978**, 11, 1265.
- Shen, M.; Mehra, U.; Ninomi, M.; Koberstein, J. K.; Cooper, S. L. *J. Appl. Phys.* **1974**, 45, 4182.
- Seymour, R. W.; Overton, J. R.; Corley, L. S. *Macromolecules* **1975**, 8, 331.
- Lilaonitkul, A.; Cooper, S. L. *Rubber Chem. Technol.* **1977**, 50, 1.